PHYSICAL REVIEW A **85**, 050307(R) (2012)

Experimental linear-optical implementation of a multifunctional optimal qubit cloner

Karel Lemr,[1] Karol Bartkiewicz,[2] Antonín Černoch,[1] Jan Soubusta,[3] and Adam Miranowicz[2]

[1]*RCPTM, Joint Laboratory of Optics of Palacký University and Institute of Physics of Academy of Sciences of the Czech Republic, Faculty of Science, Palacký University, 17. listopadu 12, 771 46 Olomouc, Czech Republic*

[2]*Faculty of Physics, Adam Mickiewicz University, 61-614 Poznań, Poland*

[3]*Institute of Physics of Academy of Sciences of the Czech Republic, Joint Laboratory of Optics of Palacký University and Institute of Physics of Academy of Sciences of the Czech Republic, 17. listopadu 12, 77207 Olomouc, Czech Republic*

(Received 30 January 2012; published 25 May 2012)

We present the first experimental implementation of a multifunctional device for the optimal cloning of one to two qubits. Previous implementations have always been designed to optimize the cloning procedure with respect to one single type of *a priori* information about the cloned state. In contrast, our "all-in-one" implementation is optimal for several prominent regimes such as universal cloning, phase-covariant cloning, and also the first ever realized mirror phase-covariant cloning, when the square of the expected value of Pauli's Z operator is known in advance. In all these regimes the experimental device yields clones with almost maximum achievable average fidelity (97.5% of theoretical limit). Our device has a wide range of possible applications in quantum information processing, especially in quantum communication. For instance, one can use it for incoherent and coherent attacks against a variety of cryptographic protocols, including the Bennett-Brassard 1984 protocol of quantum key distribution through the Pauli damping channels. It can be also applied as a state-dependent photon multiplier in practical quantum networks.

DOI: 10.1103/PhysRevA.85.050307 PACS number(s): 42.50.Ex, 03.67.−a

Introduction. One of the most fundamental laws of nature, the so-called no-cloning theorem, states that an unknown quantum state cannot be perfectly copied. This fact has an imminent impact on quantum information processing. For instance, it allows designing inherently secure cryptographic protocols [1] or assures the impossibility of superluminal communication [2]. Although perfect quantum copying is impossible, one can still investigate how well such an operation can be approximated within the limits of physical laws. Despite some very intense research in this domain, many aspects of state-dependent quantum cloning have not yet been fully investigated.

Quantum cloning is one of the most intriguing topics in quantum physics. It is important not only because of its fundamental nature but also because of its immediate applications to quantum communications, including quantum cryptography. Similar to other important quantum information processing protocols, quantum cloning has undergone considerable development over the past two decades. The first design of an optimal cloning machine was suggested by Bužek and Hillery [3]. The cloner is called optimal when it gives the best results allowed by quantum mechanics. Moreover universal cloning (UC) should operate equally well for all possible qubit states [4–8]. In contrast, limiting cloning to a specific subset of qubit states, one can achieve a more precise cloning operation. A prominent example of this situation is phase-covariant cloning (PCC), where only qubit states with equal superposition of $|0\rangle$ and $|1\rangle$ are considered [9–15].

In this Rapid Communication we address a question that is interesting from both conceptual and practical points of view: how well can a quantum state be cloned if some *a priori* information about the state is known? Theoretical investigation of this issue led to quantifying the information known about the cloned state in terms of axially symmetric distributions on the Bloch sphere [16]. This class of distributions contains an important subclass of distributions which are mirror symmetric with respect to the equatorial plane (see Fig. 1). It is therefore convenient to define mirror phase-covariant cloning (MPCC) as a strategy for cloning states with this kind of *a priori* information [17].

We hereby present an implementation of the MPCC, and we also demonstrate that the same setup can be used for optimal cloning in other prominent regimes, such as universal cloning and phase-covariant cloning. We show that the assumptions regarding the symmetry of the set of qubits cloned in an optimal way by the MPCC can be relaxed to include a wider class of qubit distributions that do not need to be axially symmetric. Finally, we demonstrate, for the example of the PCC for an arbitrary polar angle on the Bloch sphere [15], that our device can be also used as an optimal axially symmetric cloner for which the mirror-symmetry condition is not necessary.

Mirror phase-covariant cloning. In our experiment we cloned the polarization state of a single photon given by

$$|\psi\rangle = \cos(\theta/2)|H\rangle + \sin(\theta/2)e^{i\varphi}|V\rangle, \tag{1}$$

where $|H\rangle$ and $|V\rangle$ are the horizontal and vertical polarizations, respectively. In accord with the original definition [17], we assume $\langle\hat{\sigma}_z\rangle^2 = \cos^2\theta_{\rm eff}$ is the only *a priori* information known about the cloned state, where $\hat{\sigma}_z$ denotes the third Pauli operator. A geometrical interpretation of the set of states of fixed $\cos^2\theta_{\rm eff}$ is shown in Fig. 1(c). It has been recently demonstrated [16] that the MPCC can also be applied to a wider class of qubit distributions $g(\theta,\varphi)$ shown in Fig. 1(d). Consequently, the optimal cloner for a set of qubits given by a distribution $g(\theta,\varphi)$ is an MPCC set for an axial angle $\theta_{\rm eff}$ defined as $\langle\cos^2\theta\rangle = \cos^2\theta_{\rm eff}$, where the angle bracket stands for averaging over the distribution. Moreover, we note that the mirror-symmetry condition can be weakened and the MPCC transformation can be used as an optimal cloning

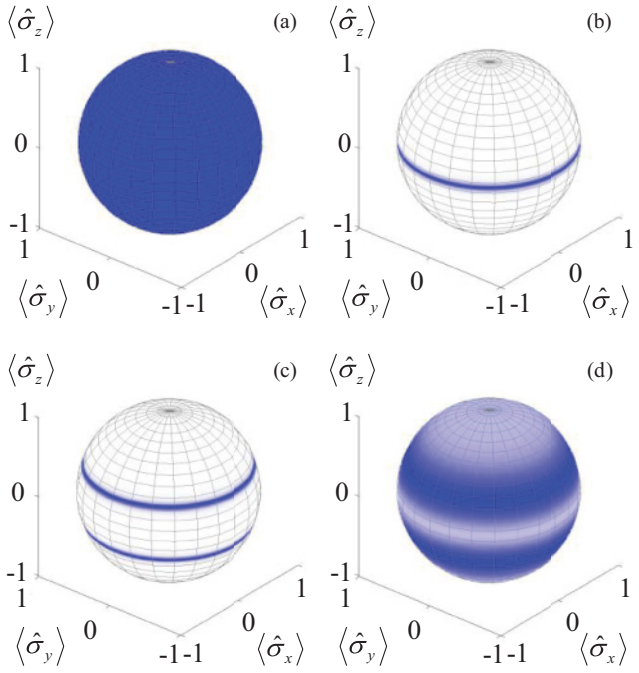

FIG. 1. (Color online) Overview of various distributions on Bloch's sphere describing *a priori* knowledge of qubits and the corresponding *optimal* cloning machines which are special cases of our multifunctional cloner: (a) uniform distribution can be cloned by the UC, (b) qubits on the equator of the Bloch sphere can be cloned by the standard PCC, (c) a union of the set of qubits for the generalized PCC and its equator-plane reflection can be cloned by the standard MPCC, and (d) any set of qubits of unknown phase symmetric about any equator plane can be cloned by the generalized MPCC.

transformation for other sets of qubits which are not axially symmetric and do not exhibit the mirror-symmetry, but rather fulfill the following conditions:

$$\int_0^{2\pi} [g(\theta,\varphi) + g(\pi-\theta,\varphi)]e^{i\varphi n}d\varphi = 0,$$
$$\int_0^{2\pi} g(\theta,\varphi)d\varphi = \int_0^{2\pi} g(\pi-\theta,\varphi)d\varphi, \tag{2}$$

where g is a distribution of qubits on the Bloch sphere and $n = 1,2$. Therefore, any MPCC optimal for some θ_{eff} is also optimal for a wider class of distributions which do not need to be axially symmetric or mirror symmetric but fulfill Eqs. (2). The above-mentioned arguments considerably broaden the usefulness of the presented device.

Experimental setup. Our experimental setup is depicted in Fig. 2. First, the cloned and ancillary photon states are prepared by means of half- and quarter-wave plates. Then the cloning operation is performed by overlapping the two photons on a special unbalanced polarization-dependent beam splitter (PDBS). Subsequently, each of the two photons undergoes polarization-sensitive filtering (transmittance τ) using the beam-divider assemblies (BDA1 and BDA2) placed in each of the output modes of the beam splitter. The PDBS employed in this scheme has different transmittances for horizontal (μ) and vertical (ν) polarizations. The transmittances should be

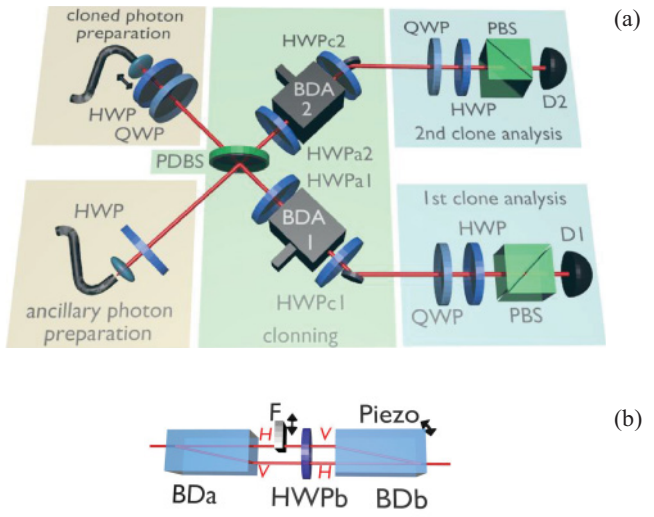

FIG. 2. (Color online) (a) Scheme of the experimental setup as described in the text. (b) Detailed scheme of the beam-divider assembly. HWP, half-wave plate; QWP, quarter-wave plate; PDBS, polarization-dependent beam splitter; BDA, beam-divider assembly; F, neutral density filter; PBS, polarizing beam splitter; D, single-photon detector; BD, beam divider.

given by

$$\mu = \frac{1}{2}\left(1+\frac{1}{\sqrt{3}}\right), \quad \nu = \frac{1}{2}\left(1-\frac{1}{\sqrt{3}}\right), \tag{3}$$

but due to manufacturing imperfections the observed transmittances of our PDBS were $\mu = 0.76$ and $\nu = 0.18$. Please note that this imperfection can be corrected without loss of fidelity through suitable filtering at the expense of a lower success rate (see Ref. [18]).

The beam-divider assembly is depicted in more detail in Fig. 2(b). It is composed of two beam dividers (BDa and BDb) used to separate and subsequently combine horizontal and vertical polarizations. A neutral density filter (F) with tunable transmittance τ is positioned between the two beam dividers so that one of the paths (polarizations) is attenuated while the other remains intact. Also a half-wave plate (HWPb) is placed between the beam dividers, swapping the polarizations and thus allowing them to be combined at the second beam divider (BDb). To control attenuation of each polarization by the neutral density filter, we envelop the beam-divider assembly by two half-wave plates (HWPa and HWPc). The beam-divider assembly is equivalent to a Mach-Zehnder interferometer, and by means of a piezo-driven tilt of one of the beam dividers, we can set an arbitrary phase shift between the two paths (polarizations).

In the ideal case, having $\mu + \nu = 1$, the setup operates as follows. A separable two-photon state $|H_1H_2\rangle$ (indices denote the mode number) is generated in the process of the type-I spontaneous parametric down conversion using a $LiIO_3$ crystal pumped by cw Kr^+ laser at 413 nm of 150-mW optical power. These photons are brought to the input of the setup via single-mode fibers. The parameters to be set for the PCC and UC regimes are just specific cases of the MPCC setting as we discuss later. For this reason we now concentrate on the MPCC setting. The polarization of the first (cloned) photon is set in

such a way that it belongs to one of the parallels of latitude on the Bloch sphere with a given polar angle θ [see Eq. (1)]. The second (ancillary) photon remains either horizontally polarized or is randomly swapped to vertical polarization. After this preparation stage the two photons are coherently overlapped at the PDBS. Depending on the polarization of the ancillary photon, we perform subsequent transformation. If the ancillary photon remains horizontally polarized, we set the half-wave plates (HWPa1 and HWPa2) in front of the beam dividers to 45° so that the vertical polarization is attenuated in both beam-divider assemblies. The level of transmittance τ of the filters F is set according to the relation

$$\tau = \frac{(1-\Lambda^2)(1-2\mu)^2}{2\mu\nu\Lambda^2}, \quad \Lambda = \sqrt{\frac{1}{2} + \frac{\cos^2\theta}{2\sqrt{P}}}, \qquad (4)$$

where $P = 2 - 4\cos^2\theta + 3\cos^4\theta$. Additionally, we also set a phase shift π between horizontal and vertical polarizations in both output modes. In the case of the ancillary photon being vertically polarized we set the half-wave plates HWPa1 and HWPa2 to 0° and this time subject the horizontal polarization to the same filtering as given by Eq. (4). Also we set the phase shift between the polarizations to zero and rotate the half-wave plates HWPc1 and HWPc2 to 45°, thus canceling the polarization swap exercised by the half-wave plates HWPb1 and HWPb2 (inside the beam-divider assemblies).

Finally, the two-photon state polarization analysis is carried out by measuring the rate of two-photon coincidences for all combinations of single-photon projections to horizontal, vertical, diagonal, antidiagonal linear, and right and left circular polarizations [19]. We can then estimate the two-photon density matrix using a standard maximum likelihood method [20].

In order to use the setup for the PCC, one just needs to set all the parameters as if performing the MPCC set for the latitude angle $\theta = \pi/2$. In the case of the PCC there is no need to randomly swap the horizontal and vertical ancillae. In this case we know the hemisphere to which the cloned states belong, so we can simply use the closer ancilla (horizontal for northern hemisphere and vertical for southern hemisphere).

A similar analysis can be carried out to determine that the setup actually performs the UC if set to the same parameters as for the MPCC with the polar angle $\theta = \arccos(\sqrt{3}/3)$. In this regime a random swap between horizontal and vertical ancillae is also required.

Experimental results. In order to verify the versatile nature of the cloner, we performed a series of measurements in three regimes: PCC, MPCC, and UC. These regimes differ just in the amount of *a priori* knowledge about the cloned state. For the PCC and MPCC we verified the theoretical prediction of maximally achievable average fidelity as a function of polar angle θ. For all polar angles (except the poles) we estimated the fidelities of both clones for four different equally distributed (on a circle defined by a fixed value of θ) input states. The observed values are depicted in Fig. 3 for the PCC and similarly in Fig. 4 for the MPCC regime. For UC (when we set constant τ of the filters at $\tau(\theta) = \tau[\arccos(\sqrt{3}/3)]$) we cloned six input states: horizontally, vertically, right and left circularly, diagonally, and antidiagonally polarized states [18]. The average fidelity obtained in the UC mode is 81.5% ± 1.2%.

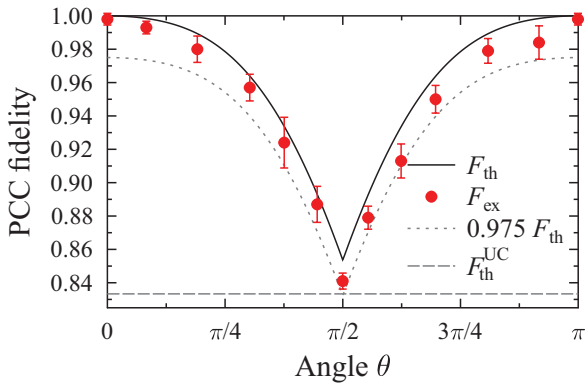

FIG. 3. (Color online) Experimental fidelity F_{ex} averaged over phase φ for the PCC regime depicted against theoretical prediction F_{th} (solid curve). The short-dashed curve indicates the fidelity drops to 97.5% with respect to the corresponding theoretical value. The theoretical fidelity F_{th}^{UC} for the UC is also depicted (long-dashed curve). For the generalized PCC the hemisphere of the cloned qubit is known (the reverse is true for the MPCC); we choose the ancilla deterministically [18] (horizontal for northern hemisphere and vertical for southern hemisphere), and we set transmittances of filters as for the MPCC tuned for the angle $\theta = \pi/2$.

The vast majority of the experimentally obtained fidelities in all regimes reached or surpassed 97.5% of their theoretical prediction, leading only to a very small experimental error.

Additional measurement of the success probability was performed for the case of MPCC. The success probability as a function of polar angle θ is depicted in Fig. 5. Note that success probability strongly depends on the splitting ratio of the beam splitter. Its theoretical prediction is given by

$$P_{th} = (1-2\mu)^2/2 + \mu\nu\tau\kappa, \qquad (5)$$

where $\kappa = (2\mu - 1)/(1 - 2\nu)$. The presented theoretical value is therefore calculated for the above-mentioned transmittances of the beam splitter used. In order to determine the success probability of the scheme we measured the coincidence rate of the setup set to perform MPCC and also the calibration coincidence rate (all the filters and beam splitter were removed). The ratio of these two rates determines the success probability calibrated for "technological losses" (inherent losses due to back reflection or systematic error of all the components) [21]. For more details see Ref. [18].

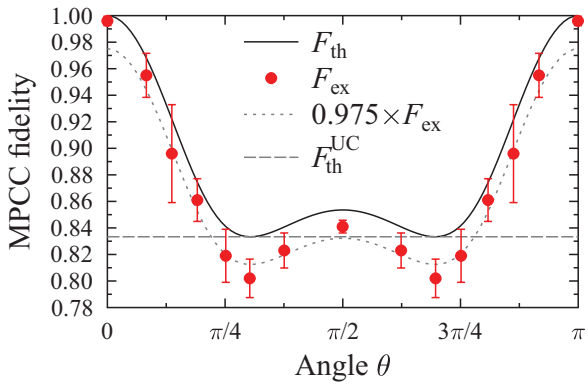

FIG. 4. (Color online) Same as in Fig. 3, but for the MPCC.

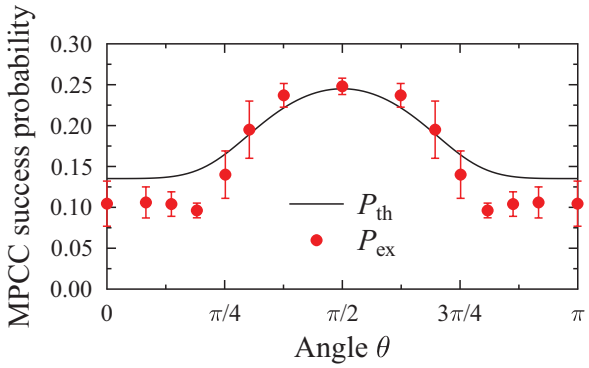

FIG. 5. (Color online) The success probability of the MPCC as a function of polar angle θ. P_{ex} denotes an experimentally determined value, and P_{th} denotes our theoretical prediction. Note that sometimes the experimental results surpass the theoretical ones; this happens at the expense of lower fidelity of the cloning process.

Conclusions. Our implementation presents a concept of a multifunctional cloner optimized for quantum communication purposes with respect to *a priori* information about transmitted states and communication channels. We have experimentally verified the versatile nature of the proposed cloner. It performs at about 97.5% of the theoretical limit for all three regimes tested (UC, PCC, and MPCC). Thus, in contrast to previous implementations, it can be used in attacks against a variety of quantum cryptographic protocols at once [22]. Some of its capabilities cannot be provided by previous cloners, especially for communication through the Pauli damping channels [18]. Potential applications of our approach might also include practical quantum networks based on state-dependent photonic multipliers or amplifiers. We therefore conclude that this device can be an efficient tool for a large set of quantum communication and quantum engineering applications requiring cloning.

Acknowledgments. K.L., A.Č., and J.S. gratefully acknowledge the support of the Operational Program Research and Development for Innovations of the European Regional Development Fund (Project No. CZ.1.05/2.1.00/03.0058) and the Operational Program Education for Competitiveness of the European Social Fund (Project No. CZ.1.07/2.3.00/20.0017) of the Ministry of Education, Youth and Sports of the Czech Republic, from the Institute of Physics of the Czech Academy of Sciences (Grant no. AVOZ10100522) and from Palacký University (internal Grant No. PrF-2011-009). A.M. and K.B. acknowledge support from the Polish Ministry of Science and Higher Education under Grants No. 2619/B/H03/2010/38 and No. 3271/B/H03/2011/40. Support from Grant No. CZ.1.07/2.3.00/20.0058 is also acknowledged.

[1] G. Van Assche, *Quantum Cryptography and Secret-Key Distillation* (Cambridge University Press, Cambridge, 2006).
[2] *Lectures on Quantum Information*, edited by D. Bruß and G. Leuchs (Wiley-VCH, Berlin, 2011).
[3] V. Bužek and M. Hillery, Phys. Rev. A **54**, 1844 (1996).
[4] V. Scarani, S. Iblisdir, N. Gisin, and A. Acin, Rev. Mod. Phys. **77**, 1225 (2005).
[5] N. J. Cerf and J. Fiurášek, in *Progress in Optics*, edited by E. Wolf (Elsevier, Amsterdam, 2006), Vol. 49, p. 455.
[6] M. Ricci, F. Sciarrino, C. Sias, and F. De Martini, Phys. Rev. Lett. **92**, 047901 (2004).
[7] W. T. M. Irvine, A. L. Linares, M. J. A. de Dood, and D. Bouwmeester, Phys. Rev. Lett. **92**, 047902 (2004).
[8] I. Ali Khan and J. C. Howell, Phys. Rev. A **70**, 010303(R) (2004).
[9] A. Černoch, L. Bartůšková, J. Soubusta, M. Ježek, J. Fiurášek, and M. Dušek, Phys. Rev. A **74**, 042327 (2006).
[10] H. Chen, X. Zhou, D. Suter, and J. Du, Phys. Rev. A **75**, 012317 (2007).
[11] L. Bartůšková, M. Dušek, A. Černoch, J. Soubusta, and J. Fiurášek, Phys. Rev. Lett. **99**, 120505 (2007).
[12] J. Soubusta, L. Bartůšková, A. Černoch, M. Dušek, and J. Fiurášek, Phys. Rev. A **78**, 052323 (2008).
[13] D. Bruß, M. Cinchetti, G. M. D'Ariano, and C. Macchiavello, Phys. Rev. A **62**, 012302 (2000).
[14] G. M. D'Ariano and C. Macchiavello, Phys. Rev. A **67**, 042306 (2003).
[15] J. Fiurášek, Phys. Rev. A **67**, 052314 (2003).
[16] K. Bartkiewicz and A. Miranowicz, Phys. Rev. A **82**, 042330 (2010).
[17] K. Bartkiewicz, A. Miranowicz, and Ş. K. Özdemir, Phys. Rev. A **80**, 032306 (2009).
[18] See Supplemental Material at http://link.aps.org/supplemental/10.1103/PhysRevA.85.050307 for more detailed technical information on the experimental setup, optimality proof of the cloners, and Pauli channels.
[19] E. Halenková, A. Černoch, K. Lemr, J. Soubusta, and S. Drusová, App. Optics **51**(4), 474 (2012).
[20] M. Ježek, J. Fiurášek, and Z. Hradil, Phys. Rev. A **68**, 012305 (2003).
[21] K. Lemr, A. Černoch, J. Soubusta, K. Kieling, J. Eisert, and M. Dušek, Phys. Rev. Lett. **106**, 013602 (2011).
[22] L. Gyongyosi and S. Imre, WSEAS Trans. Commun. **9**, 165 (2010).